The 3rd Workshop on Integration of EFD and CFD

EFD/CFD Hybrid Analysis of Internal Flow Phenomena in Turbomachinery

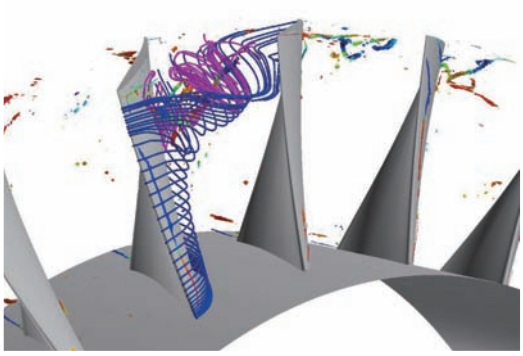

YAMADA Kazutoyo
(Kyushu University)

FURUKAWA Masato
(Kyushu University)

KIKUTA Hiroaki
(Graduate School of Kyushu University)

Introduction

Vortex breakdown

- EFD/CFD hybrid analysis revealed that the tip leakage vortex in compressor breaks down at near-stall
- EFD (reliable) → validation data, boundary condition
- CFD (visualization technique) → vortical flow structures inside passage

Key point : unsteady, but stable (not transient) ⟶ statistical processing

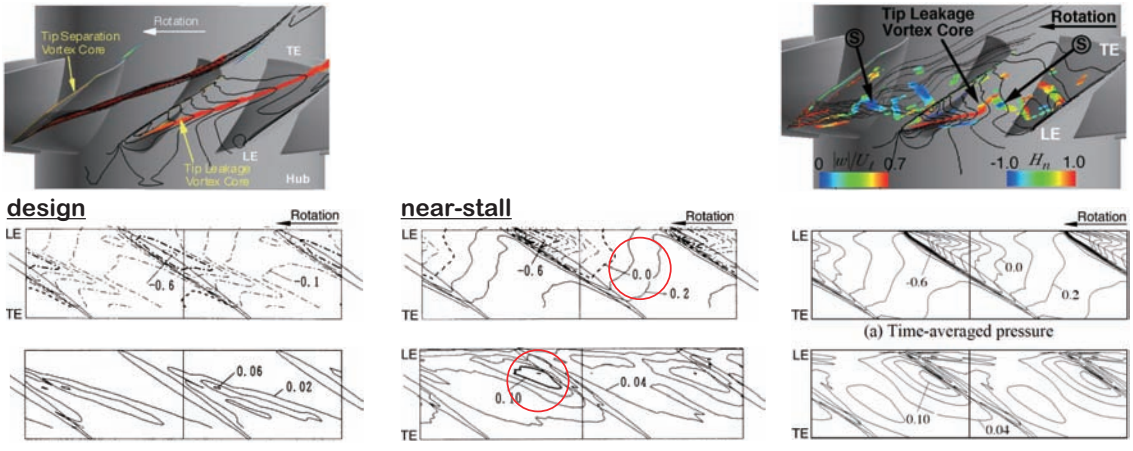

Introduction

Rotating Stall

… Anomalous flow phenomenon at low flow rate condition in turbocompressor
Stall region (stall cell) arises partially, and is circumferentially propagated and rotates in annulus compressor cascade

{ (1) Abrupt decrease in the pressure rise (,which limits the operating range)
{ (2) Blade vibration, and possibly fatigue failure of blade due to repeated load

Prediction and control of rotating stall are necessary for advanced compressor

➡ **Study on rotating stall inception in compressors**

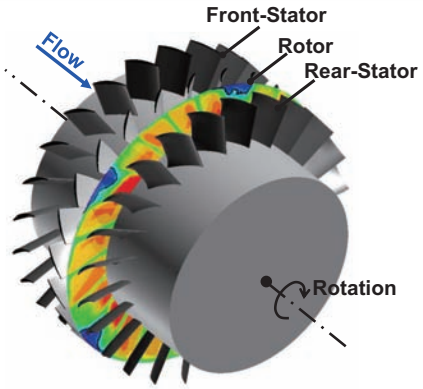

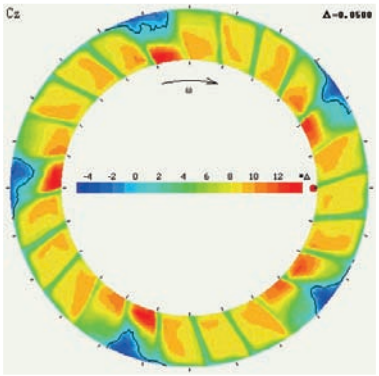

Rotating stall inception in axial compressors

- **Spike-type stall inception**
  - ➢Short-length-scale disturbance of 1～2 rotor pitch
  - ➢Rotate at 70～80% of rotor speed
  - ➢Possibly-caused by local separation near tip

- **Modal-type stall inception**
  - ➢Long-length-scale disturbance comparable to circumferential length of compressor
  - ➢Rotate at 1/4～1/2 of rotor speed
  - ➢1D model

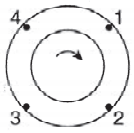

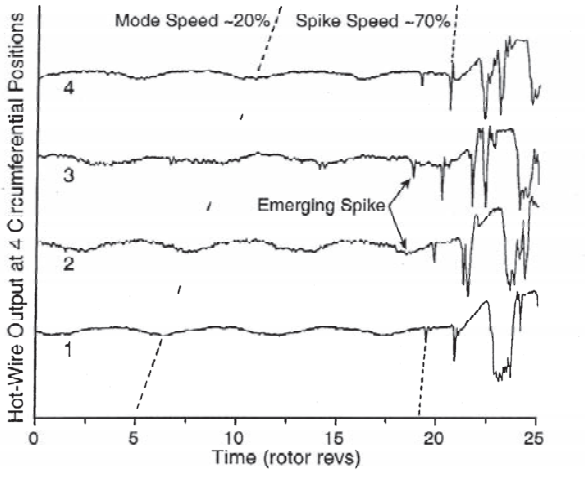

e 7 Short-length-scale event in a low-speed compressor (Day & Freeman 1994).

Spike-type stall inception and clearance flow（CFD）

●Vorticity distributions near the tip in axial compressor rotor

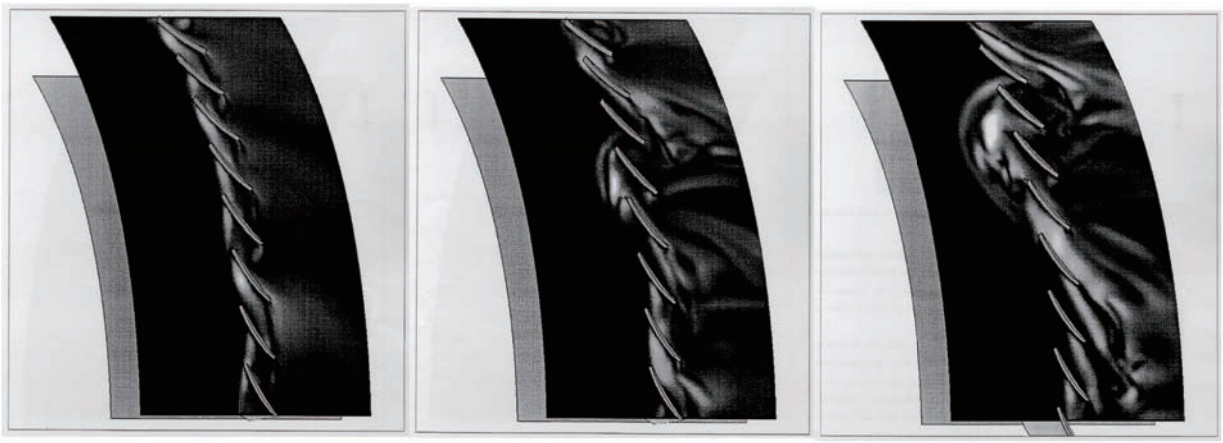

●Hoying et al. (1999):

ASME J. of Turbomachinery, Vol. 121, pp. 735-742.

Spike-type stall inception and clearance flow（CFD）

●Model for spike-type stall inception

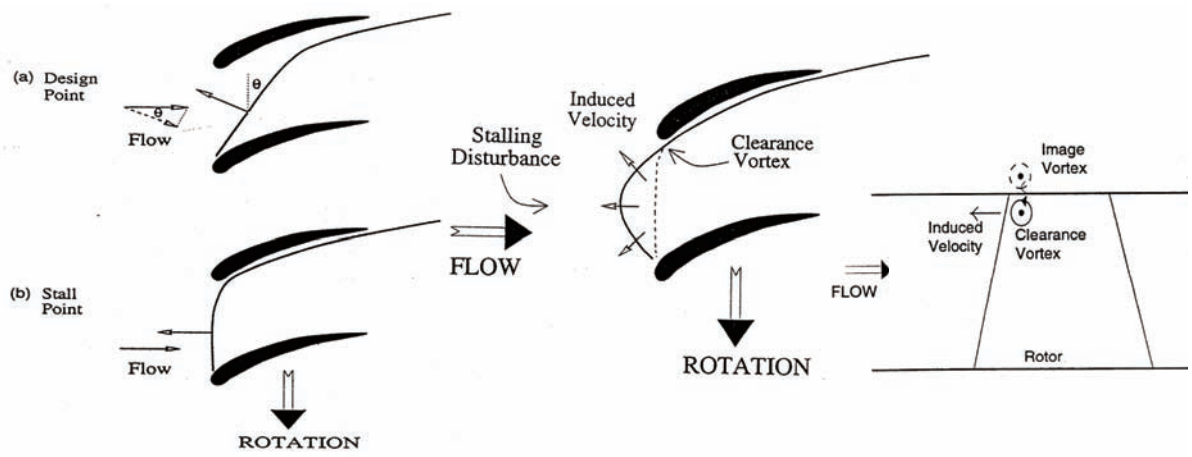

●Hoying et al. (1999):

ASME J. of Turbomachinery, Vol. 121, pp. 735-742.

Flow structure in mild stall (prior to deep stall)

●Rotating stall cell = tornado-type separation vortex

Inoue et al.（2000）- unveiled the structure of rotating stall cell by EFD

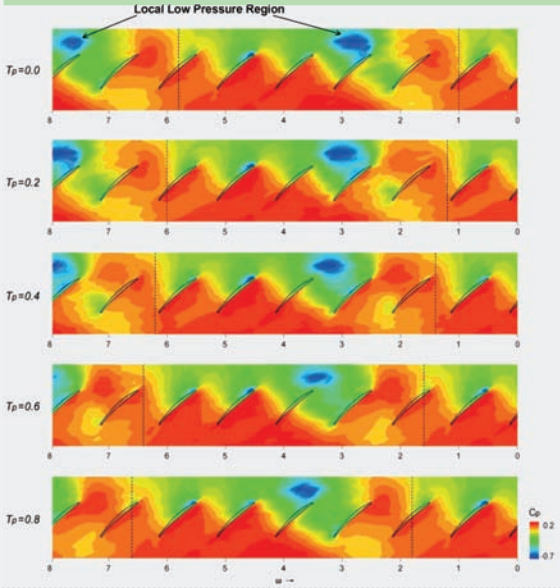

- 14 pressure transducers axially mounted on the casing
- 5 stall cells rotate at constant speed (in stable condition)

↓

- relative position of stall cell can be calculated as well as that of rotor blade

↓

Double-phase-locked averaging technique

Flow structure in mild stall (prior to deep stall)

●Rotating stall cell = tornado-type separation vortex

Inoue et al.（2000）- unveiled the structure of rotating stall cell by EFD

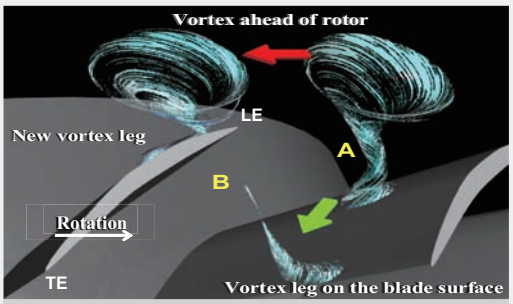

- part-span stall near rotor tip
- tornado-type separation vortex on the suction surface, which is linked with the casing wall
- a leading-edge separation occurs at the next blade tip with the approach of the vortex (propagation)

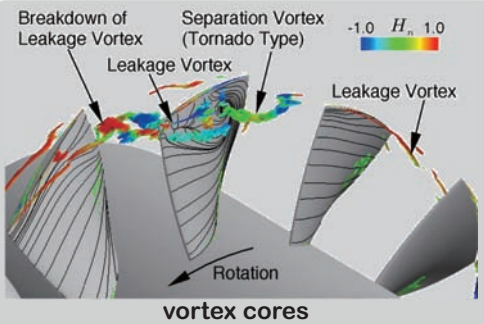

vortex cores

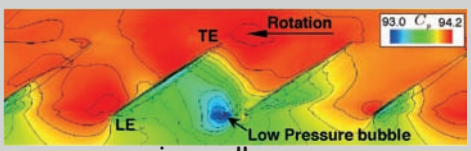

casing wall pressure

CFD results

Mechanism for this stall inception remains unclear

Goal

To clarify inception process of rotating stall in turbocompressors
(including rotating instability that appears and disappears)

(1) a low-speed research compressor (simulating compressor middle stage)

(2) a compact-size centrifugal compressor with vaneless diffuser for automotive turbocharger

EFD/CFD hybrid flow analysis

- Experiment (EFD) : Casing wall pressure and internal flow measurements
- Numerical simulation (CFD) : DES (Detached-Eddy Simulation)

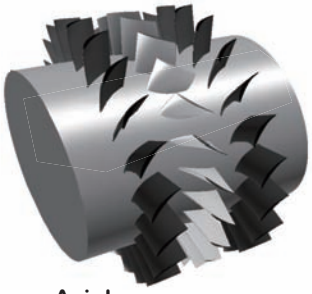

Axial compressor

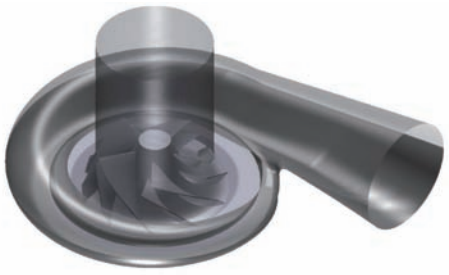

Centrifugal compressor

Low speed axial compressor

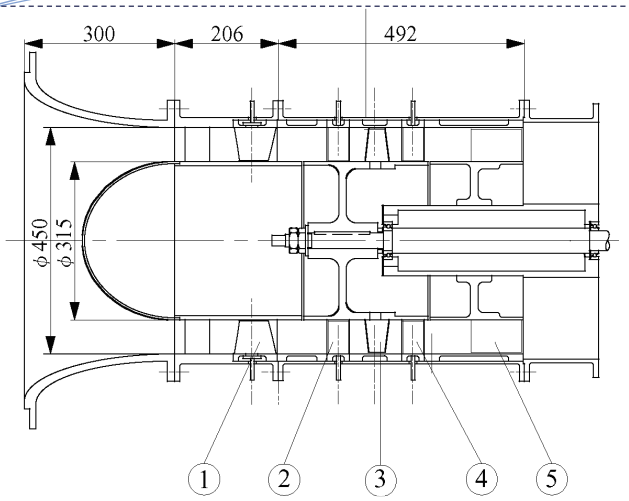

1	Inlet Guide Vane
2	Front Stator
3	Rotor
4	Rear Stator
5	Outlet Guide Vane

Rotor Blade Number	24
Stator Blade Number	22
Casing Inner Diameter	450 mm
Hub/Tip Ratio	0.7
Rotor Chord Length	50.1 mm
Tip Clearance (Chord/Tip Ratio)	0.5 mm (1%)

Condition at Design Point

Rotational Speed : 1,800 rpm

Flow Rate Coef ϕ : 0.500
(normalized by rotor tip speed)

Total Pressure-rise Coef ψ : 0.43
(normalized by dynamic pressure based on rotor tip speed)

Rotating stall inception in axial compressor (EFD)

Performance curve

mild stall
(tornado-type
separation vortex)

stall inception

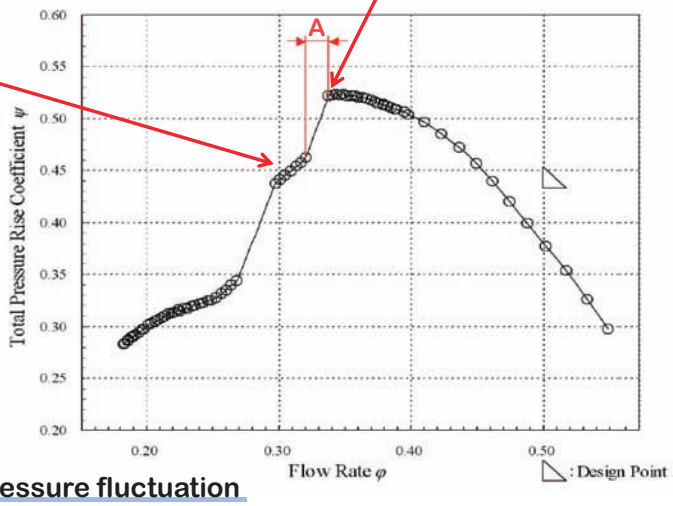

Time history of casing wall pressure fluctuation

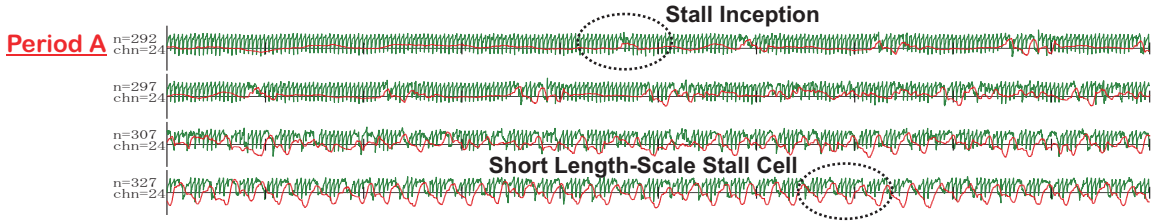

Variation of flow field near stall (EFD)

Internal flow & casing wall pressure measurement

(investigation of flow field variation down to near-stall)

design~near-stall

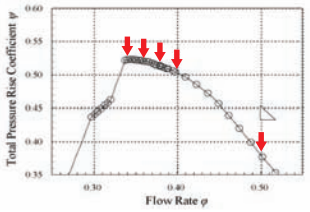

② casing wall pressure measurement
(high-response pressure sensor)

① internal flow measurement
(hot wire anemometer)

Turbulence intensity : $TL = \sqrt{\frac{1}{3}\left(\overline{C_s'^2} + \overline{C_n'^2} + \overline{C_b'^2}\right)} \Big/ u_t$

$C_s'^2$: stream-wise component
$C_n'^2$: yaw-wise component
$C_b'^2$: pitch-wise component
u_t : tip speed

Pressure variance : $P_d = \overline{p'^2} / q_t^2$

p' : pressure fluctuation
q_t : dynamic pressure based on tip speed

Near-stall flow field（EFD）

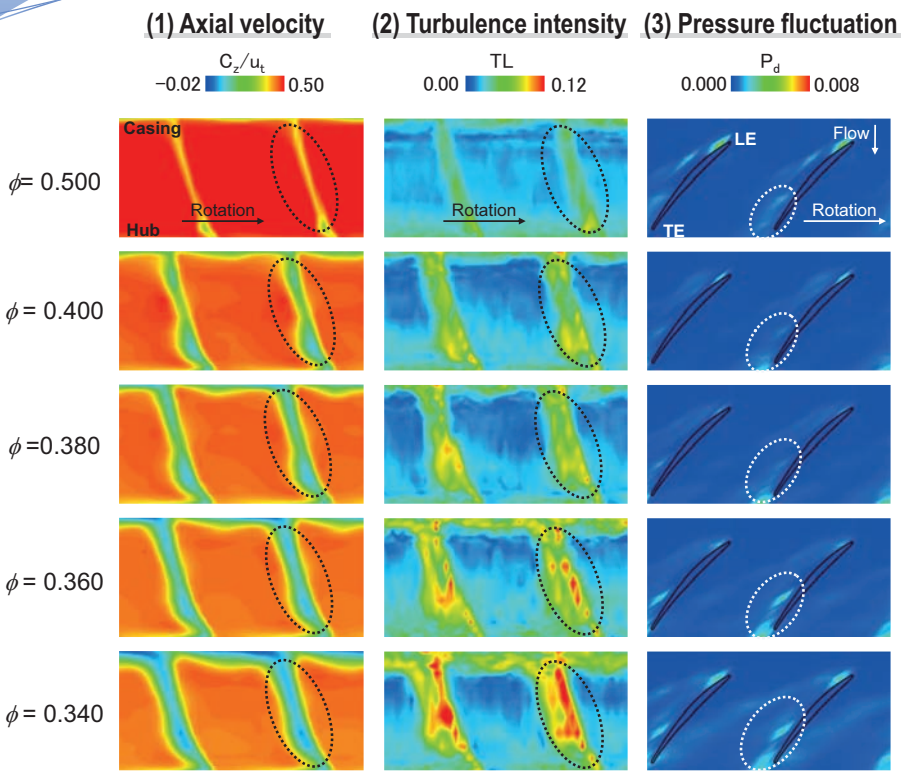

design～near-stall

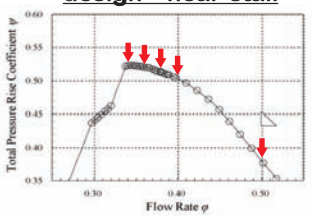

(1) unsteadiness by tip leakage vortex becomes evident with decreasing flow rate

(2) unsteadiness in suction boundary layer is developing as well

(3) suction boundary layer separation around the trailing edge

Rotating stall inception（EFD）

Casing wall pressure measurement by synchronous field measurement

（for investigation of unsteady flow phenomena at stall inception）

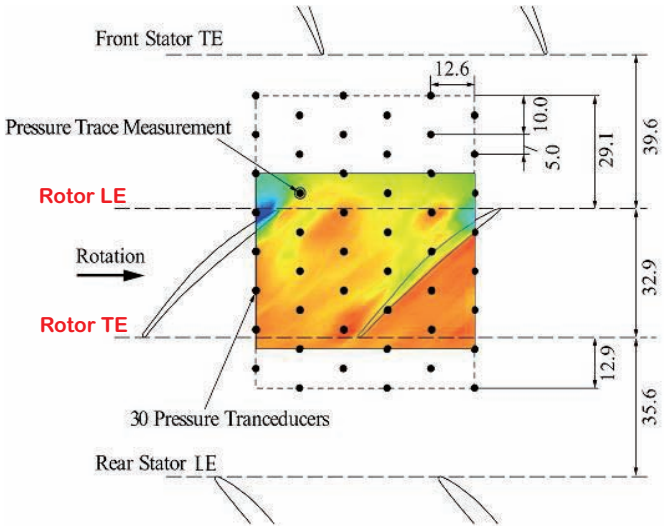

Rotating stall inception

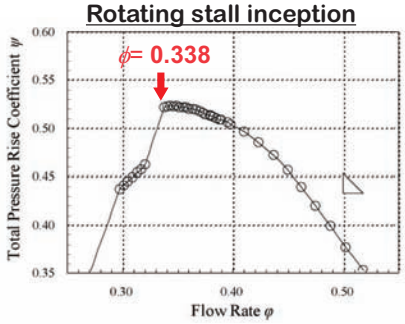

Pressure coefficient :

$C_p = (P_w - P_{0i})/q_t$

P_w : at wall　　P_{0i} : in inlet chamber

q_t : dynamic pressure based on tip speed

●Synchronous Field Measurement●

・mounted high-response pressure sensor of 30（Kulite XCS-062）

・All the sensors measures at the same time

・time-space interpolation

Casing pressure at rotating stall inception (EFD)

(1) stall inception -1

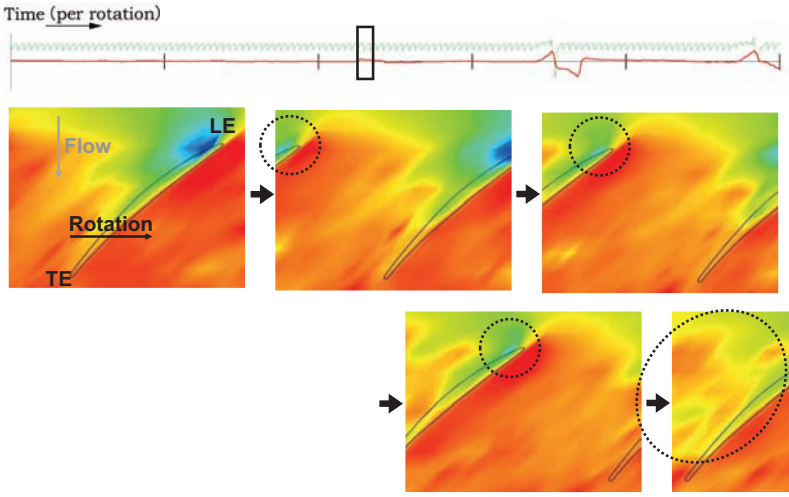

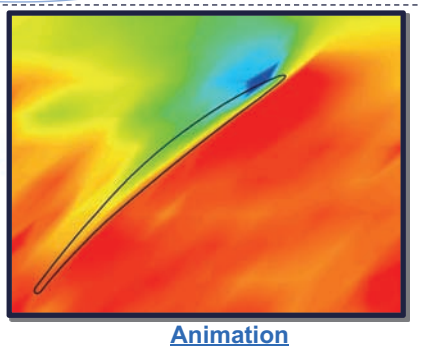

Animation

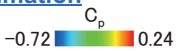

- a low pressure region near LE disappearing
  - ··· reduction in blade loading near tip
    disappearance of tip leakage vortex

→ LE separation ?

Casing pressure at rotating stall inception (EFD)

(2) stall inception -2

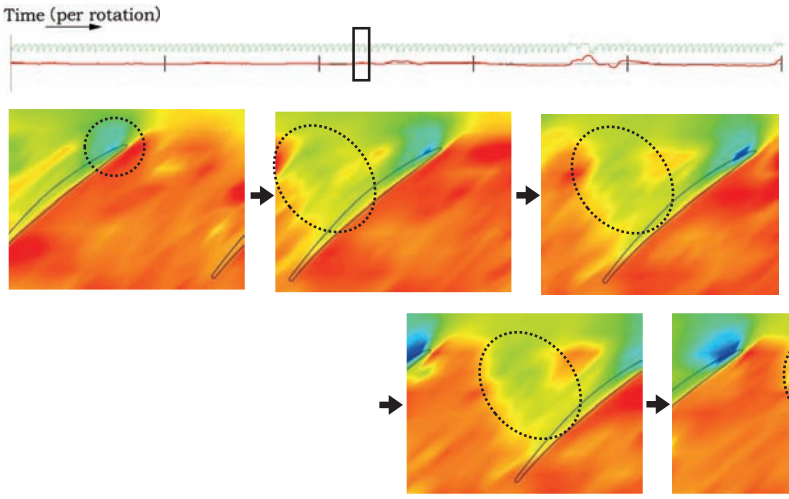

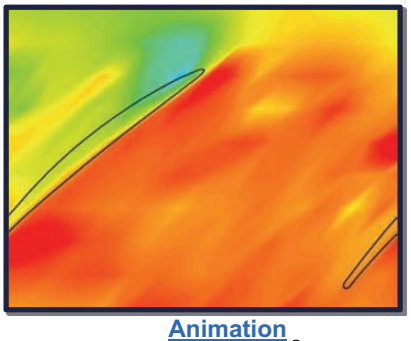

Animation

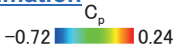

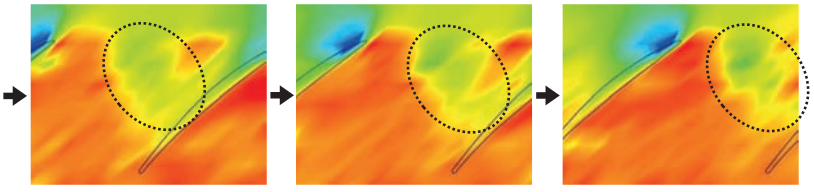

- a low pressure region near LE disappearing
- another low pressure region linked to blade suction moving to the next blade LE

→ Tornade-type separation vortex ?

Casing pressure at rotating stall inception（EFD）

(3) stall inception -3

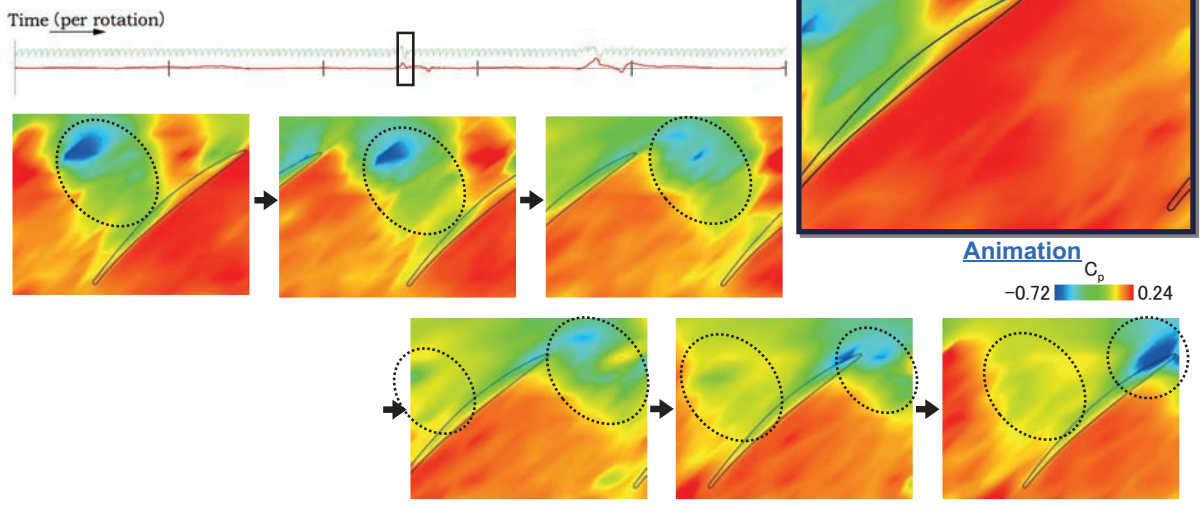

- the low pressure region linked to blade suction moving to the next blade LE
- the low pressure region transfers to the next blade after interacting with LE of the next blade (the low pressure region reappears near LE at that blade)

➡ The leading edge separation develops to the tornado-type vortex (stall cell) ?

Numerical method

◆ **Descretization**

Finite Volume Method (cell-centered type)

◆ **Numerical flux**

Roe scheme + 3rd order MUSCL

◆ **Time integration**

Euler implicit method (a point Gauss-Seidel relaxation method)
Newton iteration

◆ **turbulence analysis method**

DES(Detached Eddy Simulation) based on k-omega model

Steady-state simulation : RANS with k-omega model

DES（Detached Eddy Simulation）

DES (Detached Eddy Simulation)

switch between RANS and LES according to length-scale
(considered as a kind of wall model for LES)

- near wall : almost impossible to set enough grid resolution for LES
  - ➢ LES fails to predict turbulent boundary layer ⇒ early stalling
  - ➢ is calculated by RANS with relatively coarse grid
- main flow region :
  - ➢ separated large-scale vortices are simulated by LES

balance prediction accuracy with computational cost

⇒ **DES based on k-omega turbulence model**

M.Strelets, “Detached Eddy Simulation of Massively Separated Flows,” AIAA Paper (2001), No.2001-0879.

k-omega model based DES

k-omega model based DES

$$\frac{\partial}{\partial t}(\rho k)+\frac{\partial}{\partial x_j}(\rho \tilde{u}_j k) = \frac{\partial}{\partial x_j}\left[(\mu+\sigma^*\mu_t)\frac{\partial k}{\partial x_j}\right]+\tau_{ij}^t\frac{\partial u_i}{\partial x_j} - \beta^*\rho\omega k \quad \cdots \text{k - equation}$$

$$\frac{\partial}{\partial t}(\rho \omega)+\frac{\partial}{\partial x_j}(\rho \tilde{u}_j \omega) = \frac{\partial}{\partial x_j}\left[(\mu+\sigma\mu_t)\frac{\partial \omega}{\partial x_j}\right]+\alpha\frac{\omega}{k}\tau_{ij}^t\frac{\partial u_i}{\partial x_j} - \beta\rho\omega^2 \quad \cdots \omega\text{ - equation}$$

convection　diffusion　production　dissipation

$$D_k = \beta^*\rho\omega k = \frac{\rho k^{3/2}}{l_{k-\omega}} \quad ;where \quad l_{k-\omega} = \frac{k^{1/2}}{\beta^*\omega}$$

replace the length-scale $l_{k-\omega}$ with a grid scale $l_{SGS} = C_{des}\Delta$ if $l_{k-\omega} > l_{SGS}$

$$l_{DES} = \min(l_{k-\omega}, l_{SGS}) \quad ;where \quad C_{des} = 1.60$$

- $l_{k-\omega} < l_{SGS}$, RANS region

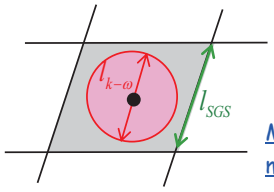

$l_{DES} = l_{k-\omega}$

Model reduces to k-omega model

- $l_{SGS} < l_{k-\omega}$, LES region

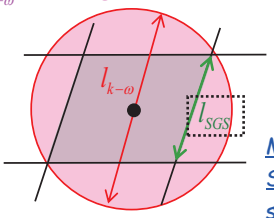

$l_{DES} = l_{SGS}$

Model reduces to Smagorinsky-like subgrid model

DES（Detached Eddy Simulation）

LES / RANS regions in DES

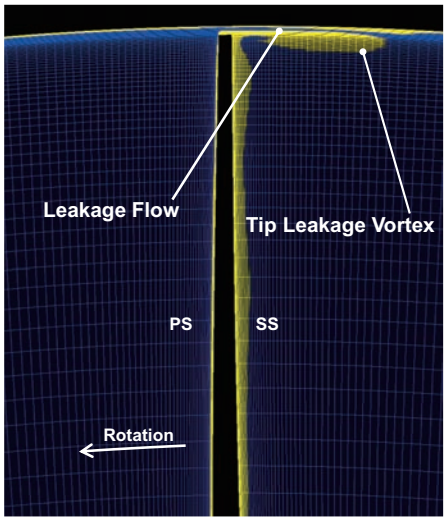

(a) axial cross section

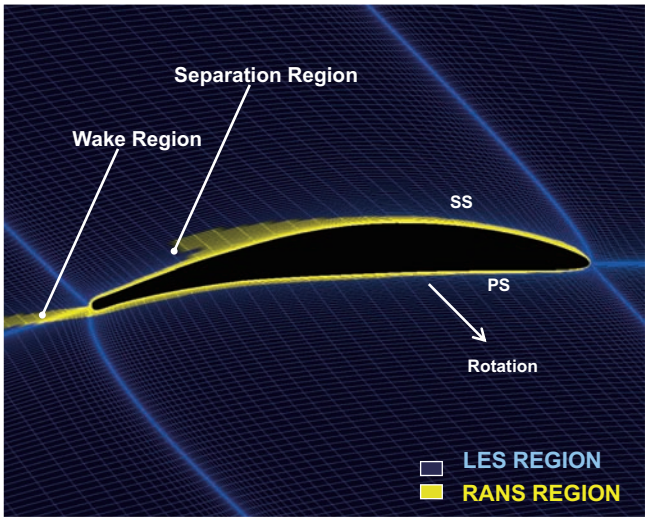

(b) radial cross section

Boundary layer, wake regions and tip leakage vortex are simulated by RANS, the other regions (separated flows) are calculated by LES

Computational grid（CFD）

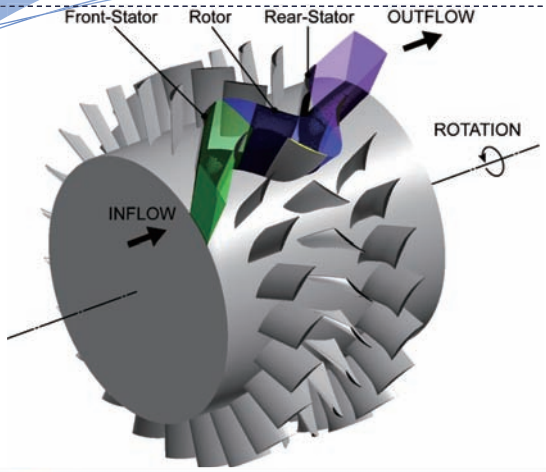

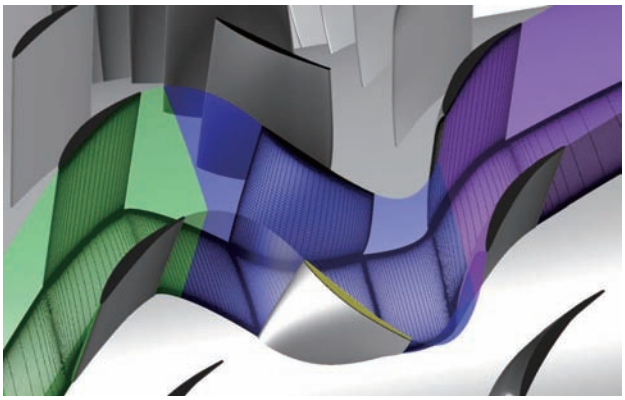

Block1 : Rotor Region	(Relative)	129 × 124 × 128 = 2,047,488 cells
Block2 : Rotor Clearance Region	(Relative)	63 × 16 × 32 = 32,256 cells
Block3 : Front Stator Region	(Absolute)	53 × 124 × 128 = 841,216 cells
Block4 : Rear Stator Region	(Absolute)	59 × 124 × 128 = 936,448 cells
1 pitch Total		3,857,408 cells
8 pitch Total		30,859,264 cells

Intelligent flow visualization

● **vortex identification based on critical point theory (Sawada, 1995)**

… When the velocity gradient tensor has one real eigenvalue and a complex conjugate pair of eigenvalues, local flow field shows helical streamline pattern, and its vortex center line is parallel to the eigenvector corresponding to the real eigenvalue.

- Determine whether each cell includes vortex center
- Quantify possibility of presence of vortex center on each cell
- Visualize vortex cores by describing iso-surface in terms of its index

● **nomalized helicity (Levy et al, 1990)**

$$H_n = \frac{\vec{\xi} \cdot \vec{w}}{|\vec{\xi}||\vec{w}|}$$

※ cosine of the angle between the vorticity and velocity vectors

$|H_n| = 1$ in streamwise vortex core

sign : direction of swirl relative to streamwise velocity component

$\vec{\xi}$: vorticity vector $\vec{w}$: velocity vector

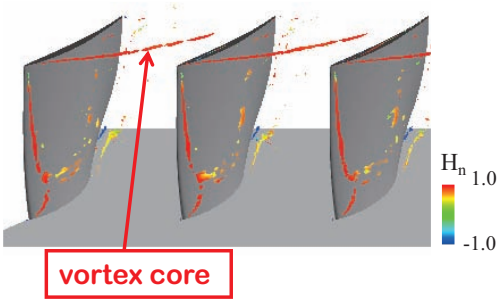

Prediction of rotating stall inception (CFD)

Performance curve

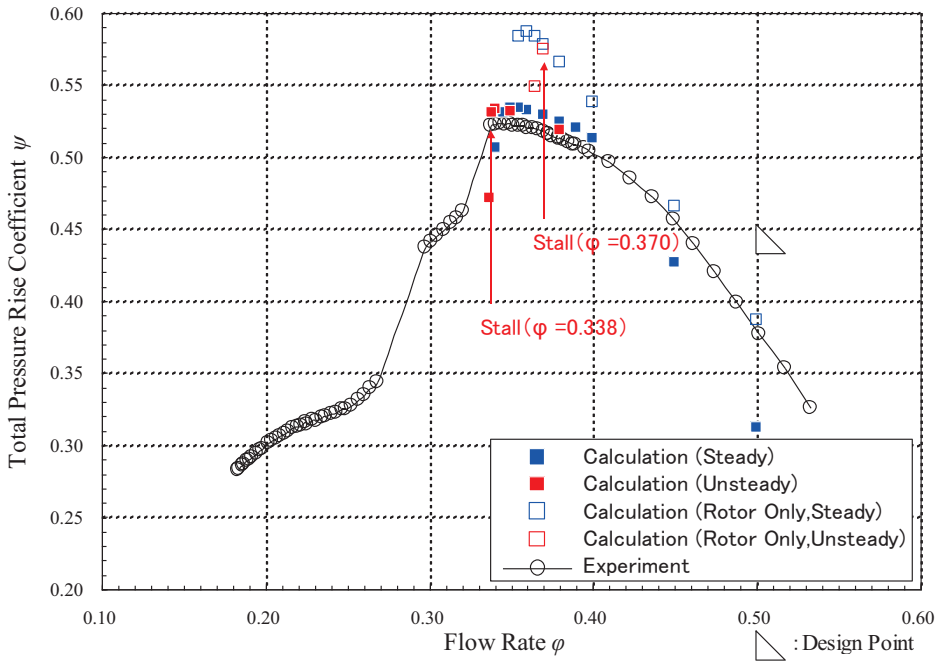

Concerning the stall point, simulation is in good agreement with experiment

Rotating stall inception process (CFD)

Casing wall pressure

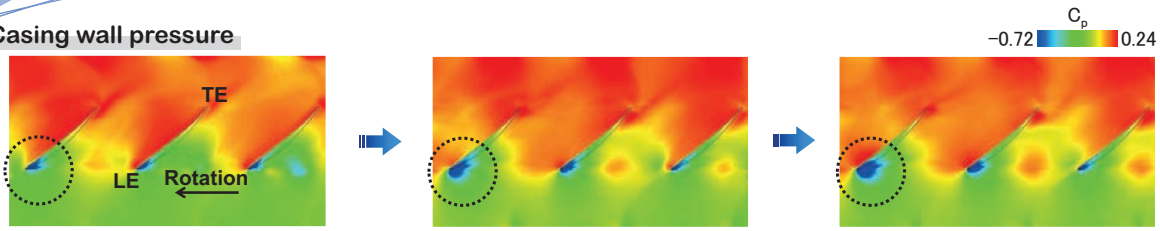

Vortical structures and streamlines

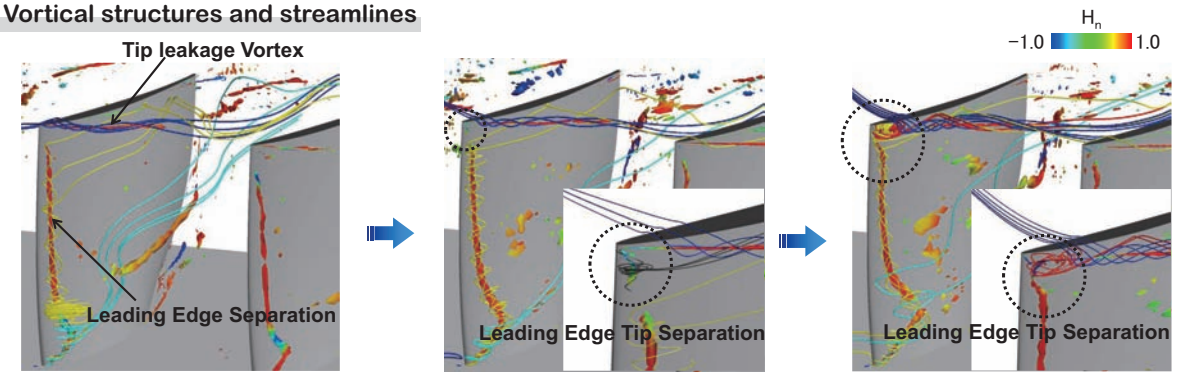

t*=551.0 t*=557.0 t*=559.0

(1) A LE separation near the tip is developing at a certain blade

(2) The LE separation vortex is linking with the tip leakage vortex, resulting in a large-scale separation vortex

Rotating stall inception process (CFD)

Casing wall pressure

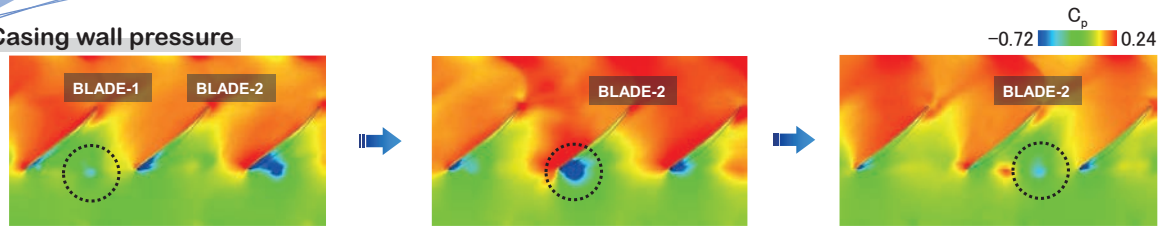

Vortical structures and streamlines

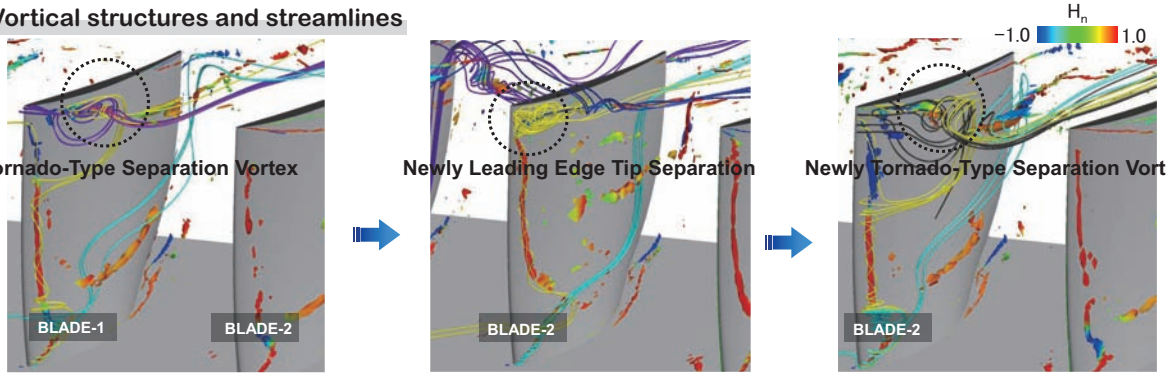

t*=551.0 t*=557.0 t*=559.0

(1) The LE separation is developing to a tornado-type vortex linked to blade suction

(2) The interaction of the tornado-type separation vortex with the next blade induces another LE separation on the next blade near the tip

(3) This is how the tornado-type separation vortex is propagating in the rotor

Rotating stall inception process (CFD)

Flow field at rotating stall inception (φ=0.337)

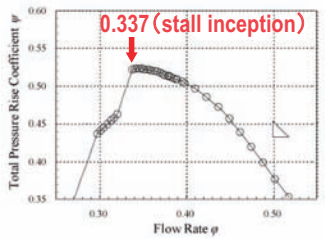

Animation of casing wall pressure

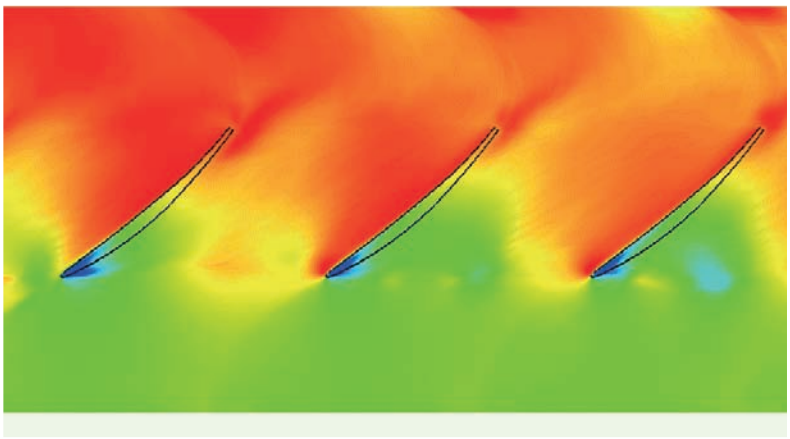

Influence of rear stator on stall inception (CFD)

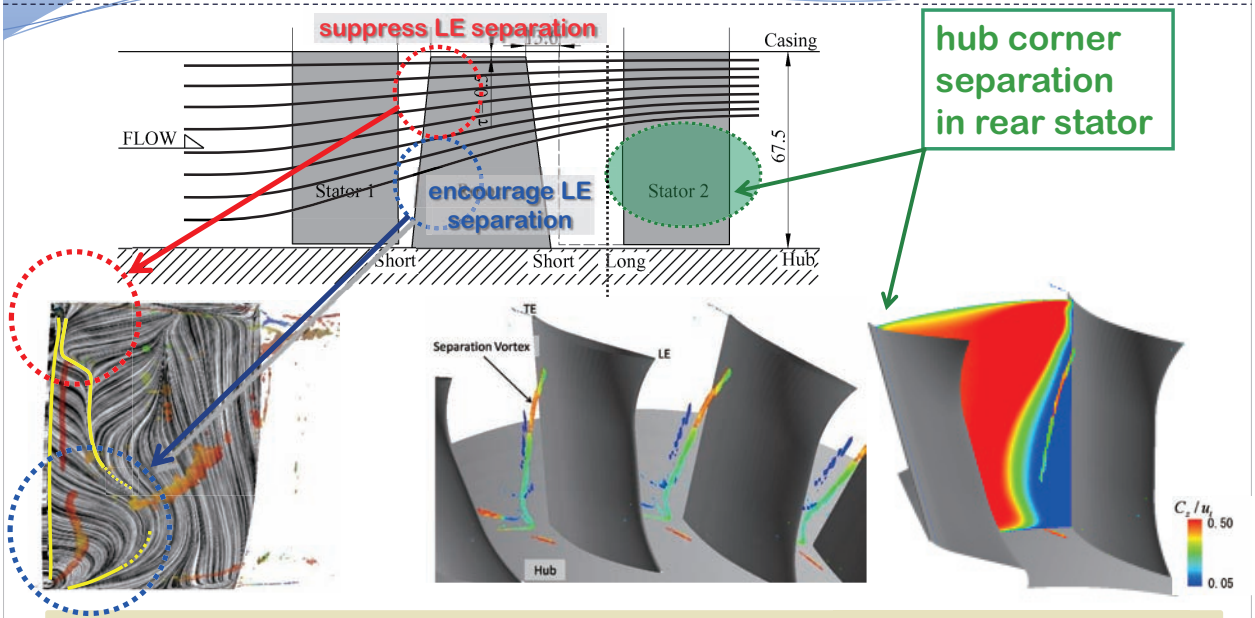

blockage effect with modal wave (hub corner separation in rear stator)

… { encourage LE separation near hub in rotor
suppress LE separation near tip in rotor

Influence of rear stator on stall inception (CFD)

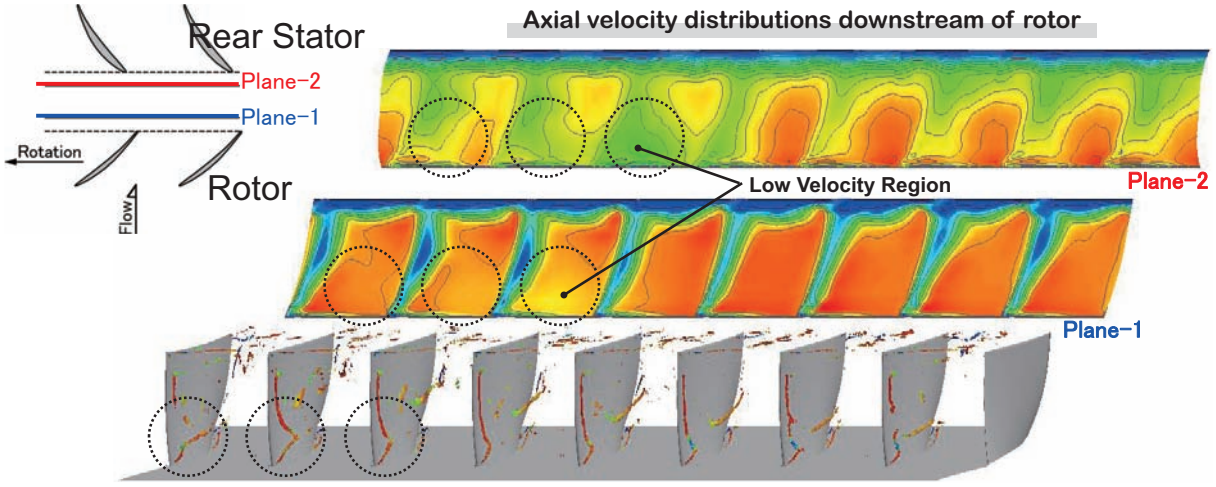

(1) axial velocity deficit region corresponds to large LE separation near the hub

(2) axial velocity deficit region rotates at 16% of rotation speed in rotor (=modal wave)

(3) modal wave is apparent downstream of rotor (originates from flow field in rear stator)

Influence of rear stator on stall inception (CFD)

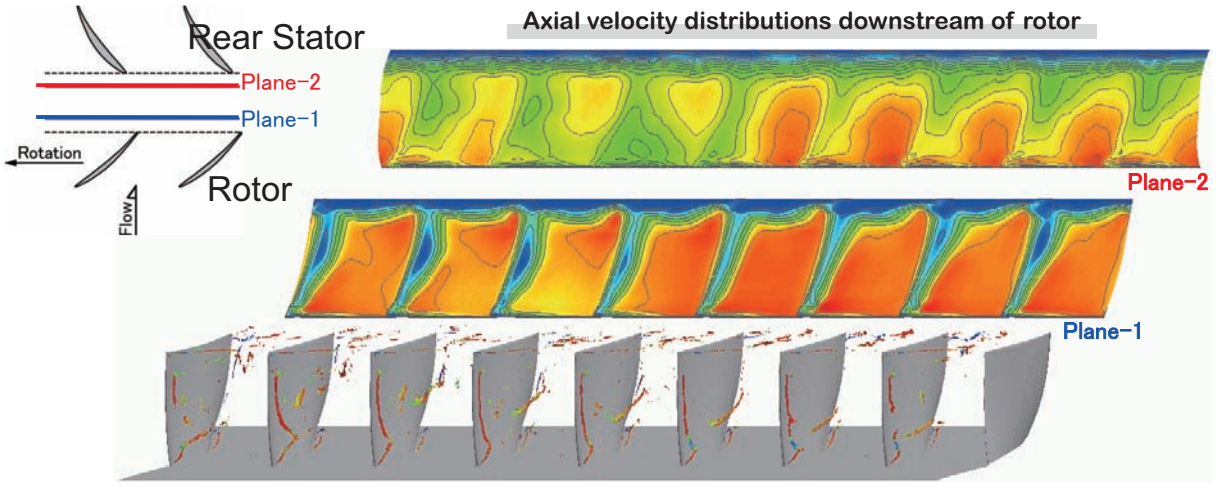

(1) axial velocity deficit region corresponds to large LE separation near the hub

(2) axial velocity deficit region rotates at 16% of rotation speed in rotor (=modal wave)

(3) modal wave is apparent downstream of rotor (originates from flow field in rear stator)

Variation in near-stall flow field (CFD)

Flow fields from design to near-stall (φ=0.500～0.338)

- LE separation is developing near the hub
- TE separation region is expanding, and merging with LE separation region
- open type separation near the hub (separation vortex shedding)

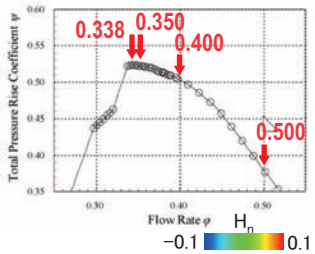

flow fields inside rotor

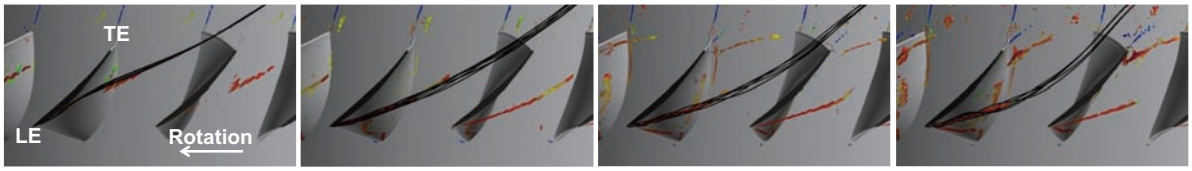

limiting streamlines on blade suction surface

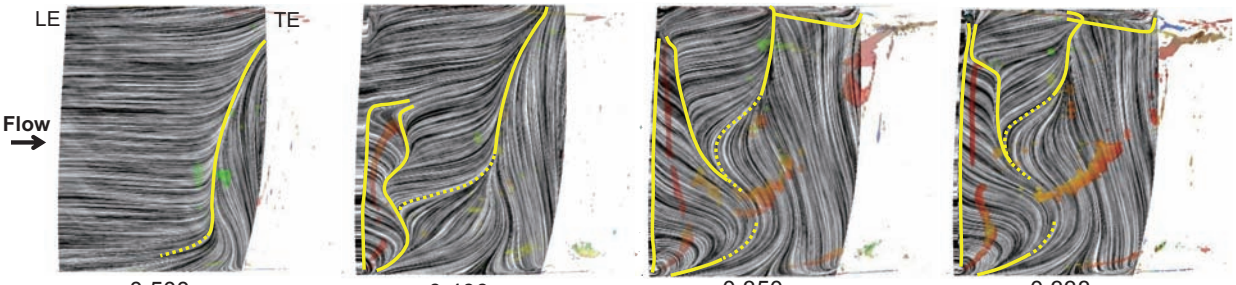

φ=0.500 (design) → φ=0.400 → φ=0.350 → φ=0.338 (near-stall)

Flow field just before stall inception (CFD)

near-stall flow field (φ=0.338)

limiting streamlines on blade suction surface

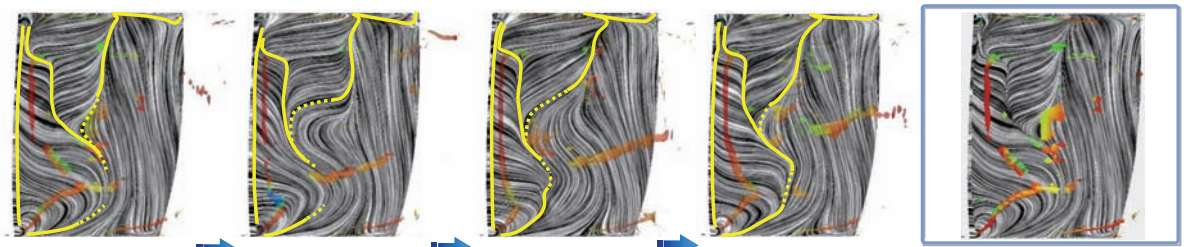

t*=406.0 → t*=412.0 → t*=418.0 → t*=424.0

Animation

- LE separation near the hub is developing with time
  → separation vortex shedding from LE separation region
- Separation vortex shedding is carried radially outward while convecting downstream

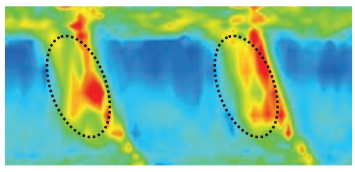

Turbulence intensity downstream of rotor (experiment)

Conclusions (rotating stall inception process in an axial compressor rotor)

- **LE separation near tip is a trigger for rotating stall inception**
  - merges with tip leakage vortex
  - develops into a tornado-type separation vortex linked to blade suction and casing wall
  - The tornado-type separation vortex moves to the next blade and interacts, and then induces the LE separation at the blade
- **Separation vortex shedding near rotor hub barely affect stall inception**
  - separation vortex shedding is carried toward casing due to centrifugal force
- **Hub corner separation in rear stator suppress the rotor stall**
  - stator should be included in simulation for accurate prediction of stall point

Issues to be addressed :

- CFD could not perfectly simulate inception process of rotating stall with respect to appearance pattern and growth rate of stall cell
- In CFD, since the LE separation can happen in every passage at the same time, some disturbances should be introduced, but what kind of disturbances is necessary and realistic?
- EFD needs the ability to measure the transient (non-periodic, random, instability nature) flow event of rotating stall inception without ensemble averaging

Future works

Key point : inception process of rotating stall is transient

↓

CFD optimized for reliable measurement data (EFD)
- casing wall pressure at transient stall inception process is available

optimization problem of unclear boundary conditions
→ Inlet distortion, differences in tip clearance and stagger angle at each blade

↓

More realistic flow phenomena can be predicted

Adjoint method
Can integrate EFD and CFD

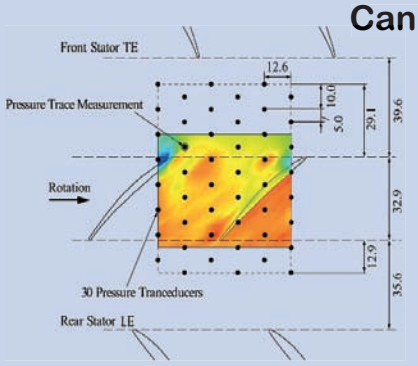

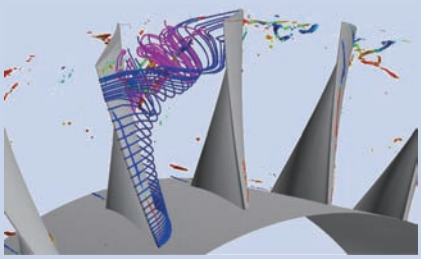

Future works

DES of full annulus of compressor (24 passages x 3) : 120 million cells (600 million degree-of-freedom)

	streamwise	spanwise	pitchwise	per passage	total amount
Rotor	130	157	129	2,632,890	63,189,360
Clearance	64	49	33	103,488	2,483,712
Front stator	54	157	129	1,093,662	26,247,888
Rear stator	60	157	129	1,215,180	29,164,320

64 cores × 12 nodes = 768 cores

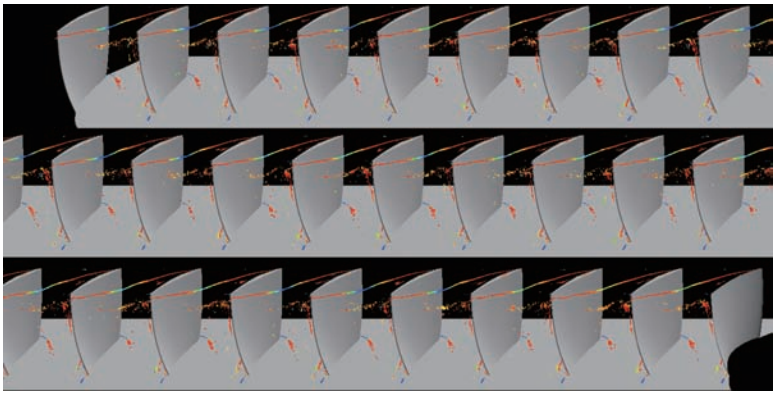

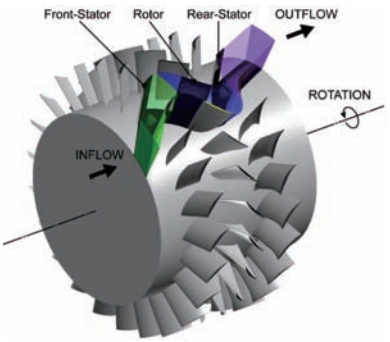

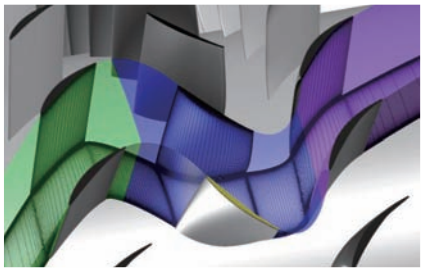

Appendix : Experimental method

Periodic Multi-Sampling

- Timing pulse synchronized with rotor rotation is generated
- Measurement data can be associated with a relative position to rotor blade

→
- Internal flow measurement (hot wire probe)
- Casing pressure measurement (pressure transducer)

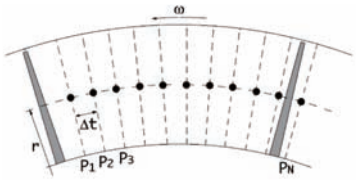

Double-Phase-Locked Averaging Technique

- Assuming that stall cell rotates at a constant speed
- Measurement data are arranged with respect to a relative position of stall cell to rotor blade
- Measurement data can be associated with a relative position to stall cell as well as rotor blade

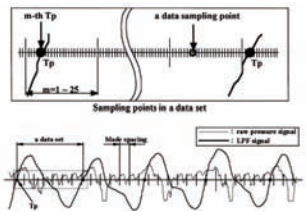

Appendix : Time-space interpolation

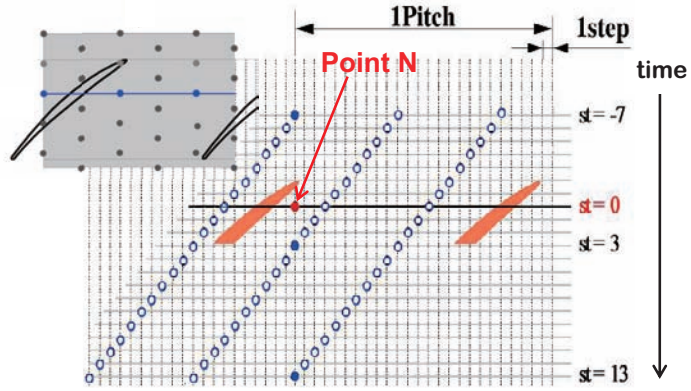

The sensors at the same axial position can obtain data at the same relative position to rotor at different times

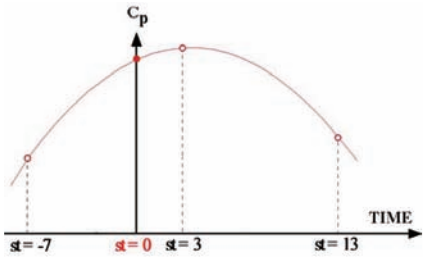

Interpolation curve in time at point N

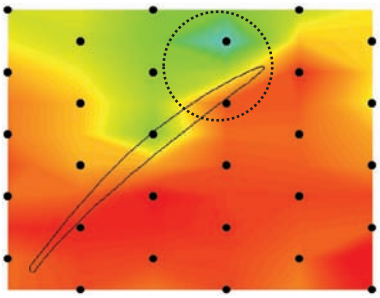

Only space interpolation

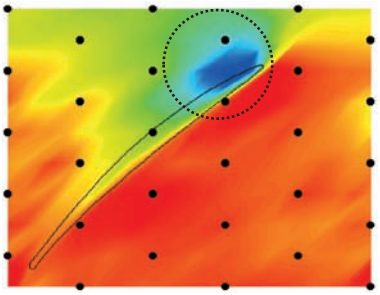

Time-space interpolation